Thermochemical Behavior of Lead Adjusting Formation of Chlorinated Aromatics in MSW Fly Ash

ARTICLE *in* ENVIRONMENTAL SCIENCE & TECHNOLOGY · JANUARY 2013

Impact Factor: 5.33 · DOI: 10.1021/es303663r · Source: PubMed

3 AUTHORS, INCLUDING:

Takashi Fujimori
Kyoto University
45 PUBLICATIONS **169** CITATIONS
SEE PROFILE

Masaki Takaoka
Kyoto University
161 PUBLICATIONS **1,046** CITATIONS
SEE PROFILE

Environmental Science & Technology

Article

pubs.acs.org/est

Thermochemical Behavior of Lead Adjusting Formation of Chlorinated Aromatics in MSW Fly Ash

Takashi Fujimori,* Yuta Tanino, and Masaki Takaoka

Department of Environmental Engineering, Graduate School of Engineering, Kyoto University, Katsura, Nisikyo-ku, 615-8540 Kyoto, Japan

Supporting Information

ABSTRACT: In this study, we examined the thermochemical role of Pb in the formation of chlorinated aromatics (aromatic-Cls) in MSW fly ash at 300−400 °C, a key temperature window for maximum yield. In the presence of lead oxide alone, aromatic-Cls formation was suppressed. One of the mechanisms of suppression was partial chlorination of PbO by an inorganic chlorine source in the solid phase, based on in situ Pb L_3-edge X-ray absorption near-edge structure (XANES) data. In contrast, quantitative GC/MS measurements revealed that $PbCl_2$ promoted aromatic-Cls formation to an extent that depends on the Pb concentration, the heating temperature, and the presence of other metal catalysts. We identified two mechanisms of aromatic-Cls formation triggered by $PbCl_2$ in MSW fly ash. First, promotion can occur by the thermochemical partial oxidation of $PbCl_2$. More specifically, real complex solid phase increases the thermochemical oxidation reactivity of $PbCl_2$, based on in situ Pb L_3-edge XANES data. Second, Cl K-edge X-ray absorption spectroscopy revealed a coexistent effect of $PbCl_2$ with other metal catalysts such as $CuCl_2$ and $FeCl_3$. The presence of $PbCl_2$ influences the balance of the bonding state of chlorine with Cu and Fe atoms at various temperatures. Thus, Pb in real MSW fly ash functions as an "adjuster" in the generation of aromatic-Cls, the nature of which depends on the lead oxide/chloride ratio and the presence of other metal catalysts.

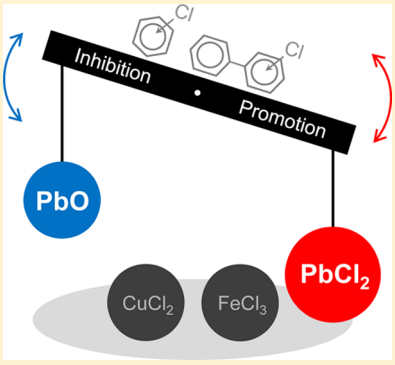

INTRODUCTION

Regarding the toxicity and resource recovery of lead, various speciation studies have reported the redox chemical state of lead in postcombustion fly ash from thermal processes such as municipal solid waste (MSW) incineration[1−6] and coal combustion.[7] According to these studies, a large amount of lead exists as chloride, oxide, or sulfide in the thermal solid phase. In contrast, lead chloride ($PbCl_2$) promotes the formation of toxic chlorinated aromatic compounds (aromatic-Cls), such as polychlorinated dibenzo-*p*-dioxins (PCDDs),[8,9] furans (PCDFs),[8,9] biphenyls (PCBs),[9] and benzenes (CBzs),[9,10] after heating of model fly ash. $PbCl_2$ in model fly ash also has a high carbon combustion rate.[11] In contrast, lead oxide (PbO) inhibits the formation of PCDDs,[9,12] PCDFs,[9,12] PCBs,[9] and CBzs.[9,13] Lead metallurgical processes can also be used to generate PCDDs, PCDFs, and PCBs.[14,15] The thermochemical behaviors of metals in the solid phase likely plays a role in aromatic-Cls formation and inhibition, which is supported by recent mechanism-based thermochemical studies of strong metal catalysts (Cu[16−18] and Fe[19−21]) and a metal inhibitor (Zn[12,22]). Previous multiaddition model studies[10,11,22−25] suggested the importance of the "coexistence (or mixture condition)" of metals. For example, a zinc-dominant solution was found to promote aromatic-Cls formation.[8,9,11,22,23] However, the presence of strong metal catalysts results in zinc acting as an inhibitor, because zinc chloride functions as a surface-coating agent and blocks the chlorination of carbon by copper or iron chlorides.[22] This suggests a thermochemical association between the chemical form of lead and aromatic-Cls formation. Lead can also promote aromatic-Cls formation, similarly to zinc, under single-addition cases.[8−11] However, the coexistence conditions of lead with strong metal catalysts such as cupric chloride and ferric chloride have not been reported. We expect that the function of lead will be affected under coexistence conditions. Because general fly ash from MSW incineration processes, namely, a complex coexistence solid phase, contains high concentrations of Pb (a few weight percent in MSW fly ash[26−29]), the contribution of lead to aromatic-Cls formation might not be negligible.

In this study, we evaluated the thermochemical behavior of lead using quantitative and X-ray spectroscopic techniques. We prepared a single-addition and coexistence-addition model fly ashes (MFAs) and real fly ashes (RFAs). Three RFAs from MSW incineration plants were analyzed by Pb L_3-edge X-ray absorption near-edge structure (XANES) spectroscopy to identify the chemical forms of lead. We tested the thermal behavior of lead chemical forms in an RFA and single-lead-addition MFAs by in situ Pb L_3-edge XANES spectroscopy.

Received: September 9, 2012
Revised: January 28, 2013
Accepted: January 31, 2013
Published: January 31, 2013

   dx.doi.org/10.1021/es303663r | Environ. Sci. Technol. 2013, 47, 2169−2176

Aromatic-Cls concentrations of MFAs under single and coexistence conditions were quantified using gas chromatography/mass spectrometry (GC/MS). Thermochemical chlorine behaviors of MFAs were analyzed using Cl K-edge near-edge X-ray absorption fine structure (NEXAFS) and were focused on the interaction between chlorine and metal atoms. Based on these results, we propose a novel thermochemical role of lead in the complex thermal solid phase during aromatic-Cls formation.

MATERIALS AND METHOD

Sample Preparation. To study the thermochemical behavior of Pb, we collected three types of RFAs (A, B, and C) from one bag filter or two electrostatic precipitators in the postcombustion zone of a municipal solid waste incinerator in Japan. We then prepared representative laboratory MFA samples. Detailed sample information is provided in Table S1 (Supporting Information). The concentrations of heavy metals, inorganic chlorine, and activated carbon (Shirasagi palm shell, 20−48 mesh; Takeda Pharmaceutical Co., Ltd., Osaka, Japan) in MFA were determined based on the compositions of the RFAs[26−29] and experimental restrictions. Metal concentrations reflected real MSW fly ash because we wanted to examine the influence of trace metals on the formation of aromatic-Cls. Referring to the components of eight RFAs in our previous study[29] and three RFAs (A, B, and C) in this study, we prepared MFA samples. The organic compounds in activated carbon were removed by heating at 500 °C for 60 min under a stream of nitrogen gas (100 mL/min). The MFA was ground in a mortar for about 10 min. We purchased SiO_2 (special grade), KCl (99.5%, special grade), $PbCl_2$ (99.0%, special grade), PbO (99.0, special grade), $CuCl_2$ (98%), and $FeCl_3$ (97%) from Nacalai Tesque Inc., Kyoto, Japan, and BN (special grade) from Wako Pure Chemical Industries, Ltd., Osaka, Japan. Details of the sample preparation were reported in our previous publication.[9,22]

GC/MS Measurements. Samples (5 g) were placed in a quartz boat contained inside a quartz tube, which was then placed in a preheated electronic furnace at 300 or 400 °C for 30 min under a flow of 10% oxygen/90% nitrogen, delivered at 50 mL/min to simulate the postcombustion zone of the municipal solid waste incinerator in Japan.[9,30] After this heating process, the concentrations of PCBs and CBzs in the sample residue and in the gas phase collected in an impinger containing 100 mL of toluene were analyzed by high-resolution GC/low-resolution MS (HP-6890/HP-5973). Pretreatment was performed to identify the chlorinated aromatic compounds according to Japanese Industrial Standards (JIS) K 0311 and 0312. For each heating experiment, analyses of PCBs and CBzs were performed in duplicate (n = 2). These results showed good reproducibility of congener profile. Median variabilities of CBzs and PCBs among all congeners were under 20%. Thus, this methodology ensured reproducibility and relatively small variability. Analytical details were reported in our previous study.[9]

Pb L_3-Edge and Cl K-Edge X-ray Absorption Spectroscopy. The chemical states of lead and chlorine were analyzed using (in situ) XANES spectroscopy. After the samples had been ground in a mortar and an agate mortar for 10 min each, they were pressed into disks. We performed Pb L_3-edge XANES spectroscopy at BL01B1 in SPring-8 (Hyogo, Japan), with the sample disk heated in a T-type in situ cell under a flow of 10% oxygen/90% nitrogen delivered at 50 mL/min. The temperature of the samples was increased from room temperature to 300 and 400 °C in a staircase pattern, as used in our previous experiments.[18] The heating rate was 5 °C/min from room temperature to 200 °C, from 200 to 300 °C, and from 300 to 400 °C. Stable conditions of temperature (200, 300, and 400 °C) wre held for 20 min. XANES spectra were measured at room temperature, 300 °C, and 400 °C. After background removal and normalization, spectral analyses were performed by a linear combination fit (LCF) using reference materials of Pb [Pb, $PbCl_2$, PbO, Pb_3O_4, $PbO{\cdot}Pb(OH)_2$, and PbS] by REX 2000 software (version 2.5.5; Rigaku, Tokyo, Japan).[2,17,18] The residual value, $R = \sum(\mathrm{XANES}_{\mathrm{measd}} - \mathrm{XANES}_{\mathrm{calcd}})^2/\sum(\mathrm{XANES}_{\mathrm{measd}})^2$, was used to evaluate the linear combination fits for the experimental spectra.

Cl K-edge NEXAFS analysis of powder samples was performed using beamlines BL-11B and BL-9A at the Photon Factory (Tsukuba, Japan). An in situ cell could not be used at the Photon Factory because of the physical restrictions of the device. Powder samples were mounted on carbon tape, and NEXAFS spectra were collected in total fluorescence yield (TFY) mode (at BL-11B) or conversion electron yield (CEY) mode (at BL-9A) under vacuum or atmospheric pressure, respectively. Details of the procedure and Cl K-edge NEXAFS analysis are described in the Supporting Information and were reported in our previous publications.[18,31]

RESULTS AND DISCUSSION

Chemical State of Pb in Real Fly Ash. The chemical states of Pb in three raw RFAs (at room temperature) were analyzed based on the spectral shapes and LCFs of the Pb L_3-edge XANES spectra. The XANES spectral shape of Pb in each RFA was similar to that of reference chloride ($PbCl_2$), as shown in Figure 1. Pb existed mainly as a combination of chloride and oxide according to the LCFs of the XANES spectra. The chemical forms of Pb in RFA-A, -B, and -C consisted of 89%, 26%, and 47% chloride and 11%, 43%, and 53% oxide, respectively (Table 1). Thus, chloride and oxide were the main Pb chemical forms. Only RFA-B contained a notable quantity of lead sulfide (31%). These results are consistent with similar previous characterizations of MSW fly ash by Pb L_3-edge XANES spectroscopy.[2,3] Overall, the three RFAs were representative mixtures of Pb chemical forms in MSW fly ash. In addition, in our previous reports, we measured the concentrations of PCBs,[29] CBzs,[29] and PCDD/Fs[34] in the same RFAs and various other real fly ashes after thermal treatment. In the following section, we compare the concentrations of PCBs and CBzs obtained for various MFAs with those obtained for the RFAs.

Thermochemical Behaviors of $PbCl_2$ and PbO. We prepared simplified MFAs admixed with $PbCl_2$ (1.0% Pb) and PbO (1.0% Pb) with KCl (10% Cl), activated carbon (3.0%), and SiO_2 (remainder), denoted as MFA-$PbCl_2$ and MFA-PbO, respectively, to examine the thermochemical behaviors of the two major Pb compounds in MSW fly ash by chemical speciation using the Pb L_3-edge XANES technique (see Table S1, Supporting Information).

MFA-$PbCl_2$ showed partial oxidation (40% PbO in Table 1) upon physical mixing at room temperature because partial oxidation of $PbCl_2$ using atmospheric oxygen gas can occur. The thermochemical behavior of Pb in MFA-$PbCl_2$ was investigated by in situ Pb L_3-edge XANES spectroscopy. We observed small changes in the spectra from room temperature to 300 and 400 °C, as shown in Figure 1. The LCF results indicated that the $PbCl_2$ composition at room temperature

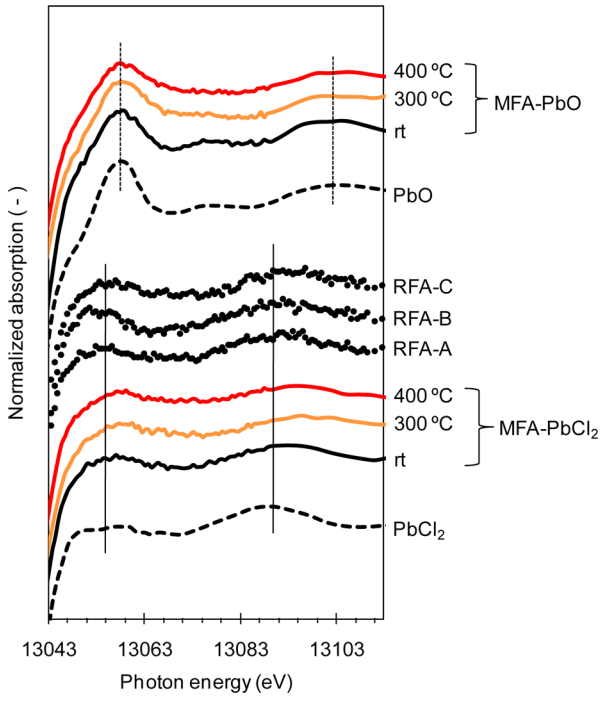

Figure 1. Pb L_3-edge XANES spectra. Dashed spectra show standard PbO and $PbCl_2$. Representative peaks of PbO and $PbCl_2$ are shown as dashed and solid vertical black lines, respectively. Three real fly ashes (RFA-A, -B, and -C) are shown as dotted spectra. Ordinary line spectra represent model fly ashes (MFA-PbO and -$PbCl_2$). Black, orange, and red represent room temperature (rt) and 300 and 400 °C, respectively.

Table 1. Lead Chloride, Oxide, and Sulfide Components (%) in Real and Model Fly Ashes Based on Linear Combination Fitting of Pb L_3-Edge XANES Spectra[a]

Pb sample		chloride (%)	oxide (%)	sulfide (%)
RFA-A	rt	89	11	
	300 °C	44	56	
	400 °C	59	41	
RFA-B	rt	26	43	31
RFA-C	rt	47	53	
MFA-PbO	rt		100	
	300 °C	25	75	
	400 °C	28	72	
MFA-$PbCI_2$	rt	60	40	
	300 °C	55	45	
	400 °C	56	44	

[a] R values indicate good fits (R = 0.006−0.018).

(60%) decreased slightly to 55−56% at higher temperatures. Our previous study showed that MFA-$PbCl_2$ (0.2% Pb) generated more aromatic-Cls after heating than an MFA without metal (activated carbon + KCl + SiO_2).[9] Although inorganic chlorides such as KCl and NaCl generally predominate in the chlorine chemical form in real fly ash, they do not efficiently promote chlorination of the carbon matrix in relation to aromatic-Cls formation.[9,31,32] Thermochemical oxidation of trace $PbCl_2$ in the model solid phase could promote the chlorination of the carbon matrix.

There is a large elemental composition gap between MFA-$PbCl_2$ and RFA. Thus, using RFA-A (which contained 89% $PbCl_2$ as the major Pb chemical form at room temperature) (Table 1), we performed in situ Pb L_3-edge XANES measurements to determine the thermochemical behavior of Pb in the real complex solid phase. Pb in RFA-A exhibited dynamic thermochemical changes. The Pb L_3-edge spectrum at room temperature (rt), similarly to that of $PbCl_2$, shifted its peak positions to higher energies, such as in the PbO spectrum, upon heating (Figure 2). The LCF results indicated that the

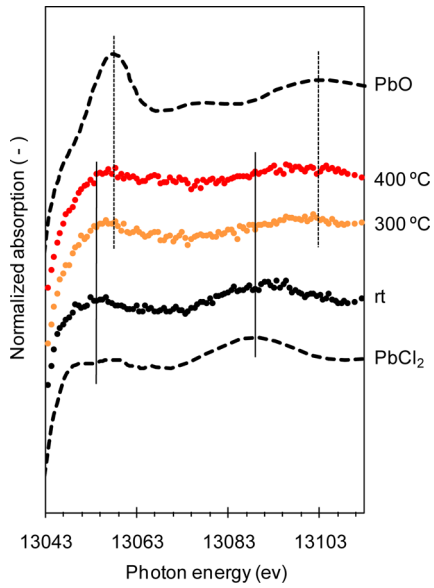

Figure 2. In situ Pb L_3-edge XANES spectra of lead chloride-rich RFA-A from room temperature (rt) to 300 and 400 °C. Dashed spectra show standard PbO and $PbCl_2$. Representative PbO and $PbCl_2$ peaks are shown as dashed and and solid vertical black lines, respectively.

89% $PbCl_2$ content in RFA-A decreased to 44−59% after heating at 300 and 400 °C, as shown in Table 1. Because the complex solid phase contributed more to the thermochemical oxidation of $PbCl_2$, the formation of aromatic-Cls was promoted. $PbCl_2$ in fly ash might function as a promoter of chlorination of the carbon matrix through its thermochemical partial oxidation. In particular, a real complex solid phase increases the thermochemical oxidation reactivity of $PbCl_2$.

After being mixed in a mortar, MFA-PbO at room temperature (rt) did not change its oxidation state as determined by LCF of the Pb L_3-edge XANES spectrum (100% lead oxide in Table 1). Heating at 300 and 400 °C lifted the characteristic spectrum dip of MFA-PbO at ∼13067 eV, as shown in Figure 1. Analysis of spectra by LCF indicated that lead oxide in MFA-PbO was partially chlorinated to 25−28% $PbCl_2$ (Table 1). The only chlorine source in the model solid phase was inorganic chloride (KCl). Thus, inorganic chloride functioned as a chlorine source for lead oxide. Previous studies reported that PbO (0.2% Pb) suppressed the effect of aromatic-Cls compared to MFA with no metal added.[9] According to our spectroscopic results, we propose the following suppression mechanism: The reduced thermochemical chlorination of carbon by inorganic chloride might be due to the suppression of aromatic-Cls resulting from the prior partial chlorination of PbO using an inorganic chlorine source in the solid phase.

Influence of $PbCl_2$ on Aromatic-Cls Formation. Based on Pb L_3-edge XANES analysis, lead chloride and oxide function as a promoter and an inhibitor, respectively, of aromatic-Cls formation, which is consistent with the thermochemical changes of lead. Thus, we selected $PbCl_2$ as

dx.doi.org/10.1021/es303663r | Environ. Sci. Technol. 2013, 47, 2169−2176

Table 2. Concentrations of CBzs and PCBs in Residues of Various Model Fly Ashes after Heating at 300 and 400 °C[a]

compound		blank[b] (ng/g)	$PbCl_2$ (ng/g)	$CuCl_2$[b] (ng/g)	CuPb (ng/g)	CuPb/Cu	$FeCl_3$[b] (ng/g)	FePb (ng/g)	FePb/Fe
After Heating Experiment at 300 °C									
CBzs	D2	18	61	230	790	**3.4**	78	330	**4.2**
	T3	0.86	43	670	680	1.0	460	400	0.87
	T4	0.33	94	5900	2400	0.41	3000	2500	0.83
	P5	0.30	92	5300	4600	0.87	4900	2900	0.59
	H6	1.1	26	2500	6700	**2.7**	3700	6100	**1.6**
	∑CBzs	21	320	15000	15000	1.0	12000	12000	1.0
	n(Cl)[c]	2.3	3.9	4.5	5.1		5.0	5.2	
PCBs	D2	0.94	4.2	4.4	6.0	**1.4**	10	7.9	0.81
	T3	7.3	24	41	31	0.75	34	21	0.62
	T4	7.5	4.1	54	42	0.77	36	23	0.63
	P5	1.2	2.0	130	40	0.31	14	14	1.0
	H6	1.0	2.4	180	47	0.26	32	23	0.72
	H7	ND[d]	0.39	320	82	0.25	36	28	0.78
	O8	ND[d]	ND[d]	430	130	0.30	49	39	0.80
	∑PCBs	18	37	1200	380	0.32	210	160	0.76
	n(Cl)[c]	3.7	3.3	6.5	6.2		5.6	5.6	
After Heating Experiment at 400 °C									
CBzs	D2	29	730	17	25	**1.4**	28	40	**1.4**
	T3	4.5	960	28	180	**6.4**	170	130	0.77
	T4	4.3	490	290	1100	**3.8**	630	890	**1.4**
	P5	4.5	91	950	2400	**2.5**	1000	1900	**1.9**
	H6	4.0	6.0	2600	1400	0.54	1800	2700	**1.5**
	∑CBzs	46	2300	3900	5100	**1.3**	3600	5700	**1.6**
	n(Cl)[c]	2.9	3.0	5.5	5.0		5.2	5.2	
PCBs	D2	1.8	1.1	2.5	3.1	**1.2**	2.9	4.3	**1.5**
	T3	30	12	3.2	6.2	**2.0**	12	17	**1.4**
	T4	29	19	6.6	20	**3.1**	17	68	**4.0**
	P5	3.2	11	5.9	11	**1.8**	27	40	**1.5**
	H6	1.2	11	5.3	35	**6.6**	72	130	**1.8**
	H7	ND[d]	2.9	15	33	**2.2**	110	160	**1.5**
	O8	ND[d]	1.3	31	42	**1.4**	96	170	**1.8**
	∑PCBs	65	59	69	150	**2.2**	340	590	**1.7**
	n(Cl)[c]	3.6	4.5	6.5	6.2		6.5	6.4	

[a]Values greater than 1.0 indicated in bold. [b]MFA-blank, MFA-$CuCl_2$, and MFA-$FeCl_3$ at 300 °C measured in our previous study.[21] [c]n(Cl) indicates the average number of chlorines. [d]ND, not detected.

a representative promoter and performed quantitative single-addition and multiaddition tests using GC/MS. We detected increased amounts of CBzs and PCBs after heating of MFA-$PbCl_2$ and then compared these findings to the results for MFA-blank (KCl + activated carbon + SiO_2 in Table S1, Supporting Information) after heating at 300 and 400 °C, as reported in Table 2 for the residual solid phase and in Table S2 (Supporting Information) for the gas phase. Although the salt KCl in MFA-blank influenced the formation of aromatic-Cls (see the Supporting Information and Table S3), $PbCl_2$ promoted thermochemical aromatic-Cls formation in the solid and gas phases more than in the case of the blank (only KCl). The concentrations of CBzs and PCBs were positively correlated with that of PCDD/Fs by using MFAs with various metal additives.[9] Thus, PCDD/Fs might be generated by $PbCl_2$ (and other metal additives) in this study. The GC/MS quantitative data set facilitated the assessment of the influence of the Pb concentration (0.2%[9] and 1.0% Pb), heating temperature (300 and 400 °C), metal species (Pb, Cu, and Fe), and coexistence with other metal catalysts. According to composition of real fly ash determined in a previous study,[28] $CuCl_2$ (0.2% Cu) and $FeCl_3$ (0.5% Fe) were added to KCl (10% Cl), activated carbon (3.0%), and SiO_2 (remainder) (called MFA-$CuCl_2$ and MFA-$FeCl_3$, respectively).

In this study, we mainly focused on the thermochemical behavior of Pb in the residual solid phase after heating because other analytical techniques such as Pb L_3-edge XANES and Cl K-edge NEXAFS spectroscopies are appropriate for solid-phase analysis and can be linked with the quantitative results by GC/MS. However, GC/MS measurements can also be used to analyze the formation of CBzs and PCBs in the gas phase (Table S2, Supporting Information). The thermochemical behavior of Pb might contribute to the formation of aromatic-Cls in the gas phase. Basically, the formation of almost aromatic-Cls in the solid phase is superior to that in the gas phase at 300 and 400 °C, according to the calculated solid/gas ratios of aromatic-Cls concentrations as reported in Table S3 (Supporting Information). Although some congeners of CBzs had the potential for volatility in the gas phase at 400 °C (Table S4, Supporting Information), most congeners of PCBs were concentrated in the solid phase even at 400 °C. This difference in solid/gas ratio was found to depend on the volatility of the aromatic-Cls. In our previous study, we reported that PCDD/Fs had the highest-level solid/gas ratios among PCDD/Fs, PCBs, and CBzs.[9] Thus, low-volatility

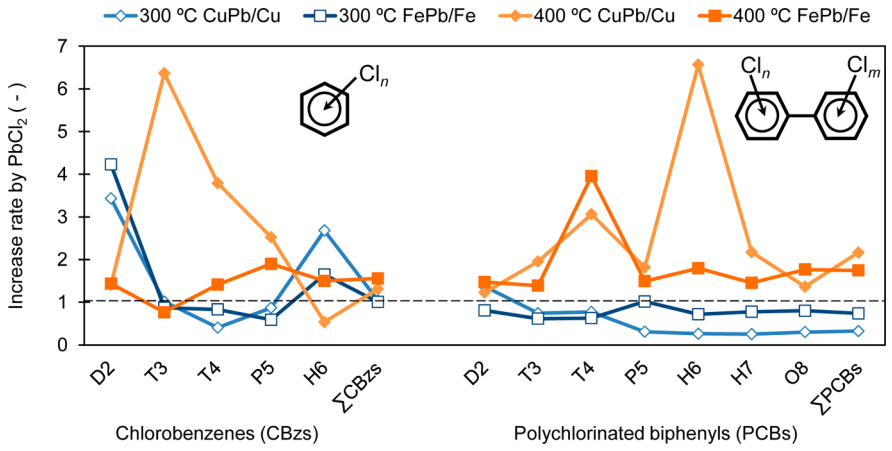

Figure 3. Mixed effect of $PbCl_2$ in the solid phase according to the concentrations of D2−H6 benzenes and D2−O8 biphenyls after heating at 300 and 400 °C.

aromatic-Cls (PCDD/Fs and PCBs) might become concentrated in the solid phase of MSW fly ash in the postcombustion zone. In contrast, the volatile behavior of CBzs was controlled by temperature in the range of 300−400 °C. From this point on, we mainly discuss the concentration data of aromatic-Cls in the solid phase as shown in Table 2.

At 300 °C, the ∑CBzs concentration of MFA-$PbCl_2$ (1.0% Pb), 320 ng/g, was higher than that of MFA-$PbCl_2$ (0.2% Pb[9]), 160 ng/g. Thus, the Pb concentration influenced CBzs formation. In contrast, ∑PCBs in MFA-$PbCl_2$ (1.0% Pb) was 37 ng/g, which did not differ significantly from the value for MFA-$PbCl_2$ (0.2% Pb[9]), 40 ng/g, after heating at 300 °C. The gas-phase concentrations also showed the same tendencies, according to a comparison of the results of this study (Table S2, Supporting Information) with our previous results.[9] PCBs formation is thought to be weakly influenced by Pb concentration. Single-ring aromatics (CBzs) were found to be more influenced by $PbCl_2$ concentration than double-ring aromatics (PCBs). Although CBzs are thought to be precursors of dioxins (PCDD/Fs and PCBs), $PbCl_2$ might not have the potential to catalyze the dimerization of CBzs from these results. However, the dimerization of other precursors such as chlorophenols might be catalyzed by $PbCl_2$, so a detailed investigation of this point needs to be performed in the future.

Temperature is important factor in the thermochemical formation of aromatic-Cls by solid-phase $PbCl_2$. MFA-$PbCl_2$ heated at 400 °C generated higher concentrations of ∑CBzs and ∑PCBs than the same MFA heated at 300 °C (Table 2): ∑CBzs =2300 ng/g (400 °C) > 320 ng/g (300 °C) and ∑PCBs = 59 ng/g (400 °C) > 37 ng/g (300 °C). Table S2 (Supporting Information) indicate that the gas-phase results exhibited the same temperature dependence (400 > 300 °C). In the solid phase, the presence of CBzs in MFA-$PbCl_2$ increased the concentration of low-chlorinated congeners such as D2, T3, and T4 after heating from 300 to 400 °C. In contrast, the concentration of high-chlorinated congeners of PCBs (T4−O8) increased in the presence of MFA-$PbCl_2$. This temperature profile of ∑CBzs concentration obtained by $PbCl_2$ (400 > 300 °C) has characteristics opposite to that of the concentration obtained by catalytic $CuCl_2$ and $FeCl_3$ (400 < 300 °C), as shown in Table 2. Although MFA-$FeCl_3$ exhibited a ∑PCBs temperature profile identical to that of MFA-$PbCl_2$, that of MFA-$CuCl_2$ differed. These temperature profiles were caused by differences in the thermochemical behaviors of the metal species.[17,18,21] At 300 °C, $CuCl_2$ showed a maximum potential to generate aromatic-Cls in the solid phase by catalytic cycle[17] and direct chlorination.[18] $FeCl_3$ changed its chemical form, and an oxychlorination reaction occurred at 300−400 °C.[21] In contrast, the CBzs and PCBs of MFA-$PbCl_2$ in the gas phase showed same temperature dependence as those of MFA-$CuCl_2$ and -$FeCl_3$ (Table S2, Supporting Information). CBzs have higher volatilities than PCBs, which implies that aromatic-Cls are more volatilized to the gas phase from the solid phase at 400 °C than at 300 °C.

Regarding the metal species, concentrations of aromatic-Cls in the solid phase were in the order (Table 2): $CuCl_2$ > $FeCl_3$ > $PbCl_2$ > blank (∑CBzs at 300 and 400 °C, ∑PCBs at 300 °C). This ranking of metal chlorides is consistent with previous studies.[8−10] The ranking of ∑PCBs at 400 °C differed: $FeCl_3$ > $CuCl_2$ ≈ $PbCl_2$ ≈ blank (∑PCBs at 400 °C). The concentrations of ∑PCBs at 400 °C were similar among $CuCl_2$ (69 ng/g), $PbCl_2$ (59), and blank (65). Table 2 shows that the average number of chlorines, n(Cl), of $PbCl_2$ ranged between the low- (blank) and high- ($CuCl_2$, $FeCl_3$) chlorinated values, excluding PCBs at 300 °C. The gas phase showed the following specific order of CBzs: $FeCl_3$ > $CuCl_2$ > $PbCl_2$ > blank. $FeCl_3$ has a more volatile character. Although CBzs were volatilized from the solid phase, the gas-phase formation of CBzs is also thought to be promoted by volatilized ferric chloride.[31]

Compared with the results of our previous study,[29] we found that MFA-$PbCl_2$ has less potential to promote the formation of ∑CBzs and ∑PCBs after heating at 300 °C than RFAs. Thus, other additional factors might be keys of promotion effects. In fact, MFA-$CuCl_2$ and MFA-$FeCl_3$ exhibited the same orders of concentrations of ∑CBzs and ∑PCBs after heating at 300 °C as RFAs. Furthermore, the coexistence of $PbCl_2$ with other metal promoters ($CuCl_2$ or $FeCl_3$) also affects the concentrations of aromatic-Cls and showed same potential to promote aromatic-Cls as RFAs. Coexistence-conditions MFA was found to be more similar in chemical composition to RFA than to MFA with one added metal chloride. The rate increase of aromatic-Cls generation is defined by one of the following formulas

dx.doi.org/10.1021/es303663r | Environ. Sci. Technol. 2013, 47, 2169−2176

$$\text{rate increase by CuPb (CuPb/Cu)} = \frac{[\text{Ar}]_{\text{CuPb}}}{[\text{Ar}]_{\text{CuCl}_2}}$$
$$\text{rate increase by FePb (FePb/Fe)} = \frac{[\text{Ar}]_{\text{FePb}}}{[\text{Ar}]_{\text{FeCl}_3}} \quad (1)$$

where $[\text{Ar}]_X$ is the concentration of aromatic-Cls (CBzs and PCBs) in the case of MFA-X. MFA-CuPb or MFA-FePb were $CuCl_2$ (0.2% Cu) or $FeCl_3$ (0.5% Fe), respectively, admixed with $PbCl_2$ (1.0% Pb), KCl (10% Cl), activated carbon (3.0%), and SiO_2 (remainder). If the rate increase was greater than 1.0, the generation of aromatic-Cls was promoted by the coexistence of $PbCl_2$. ∑CBzs at 300 °C maintained their concentration in mixtures of $PbCl_2$ with $CuCl_2$ and $FeCl_3$; that is, CuPb/Cu and FePb/Fe = 1.0 (Table 2). The rate increases of the D2 and H6 congeners of CBzs at 300 °C were over 1.0 in MFA-CuPb (3.4 and 2.7) and -FePb (4.2 and 1.6), as shown in Figure 3. The gas phase exhibited similar rate increases of the D2 and H6 congeners of CBzs (Table S2, Supporting Information), which suggests the volatilization of CBzs from the solid phase. In particular, the H6 congener of CBzs (hexachlorobenzene) is involved in persistent organic pollutants (POPs). Thus, toxic POPs were increased by the coexistence of $PbCl_2$ with metal catalysts at 300 °C. ∑PCBs and most congeners of PCBs at 300 °C were inhibited by the coexistence of $PbCl_2$ with $CuCl_2$ (CuPb/Cu < 1.0) and $FeCl_3$ (FePb/Fe < 1.0), as shown in Table 2. However, the coexistence inhibition effects of $PbCl_2$ on PCBs were milder than those of $ZnCl_2$ in our comparable previous data set at 300 °C.[22] In the gas phase, the rate increases of the T3, T4, P5, and H7 congeners of PCBs were >1.0 upon heating of MFA-FePb at 300 °C, although the value for ∑PCBs was <1.0 (Table S2, Supporting Information). Excluding the D2 and H6 congeners of CBzs, the concentration of CBzs was constant, and mild inhibition of PCBs was caused by the coexistence of $PbCl_2$ at 300 °C.

In contrast, the rate of aromatic-Cls formation after 400 °C heating of MFA-CuPb and -FePb increased, as shown in Figure 3. ∑CBzs and ∑PCBs in MFA-CuPb at 400 °C generated 1.3- and 2.2-times more aromatic-Cls, respectively, than those in MFA-$CuCl_2$ (Table 2). Almost all congeners of CBzs and PCBs in MFA-CuPb at 400 °C showed rate increases over 1.0, excluding the H6 congener of CBzs. Relatively high rate increases (CuPb/Cu > 2.0) were detected for the T3, T4, and P5 congeners of CBzs and the T4, H6, and H7 congeners of PCBs at 400 °C (Figure 3). Thus, $PbCl_2$ functioned as a promoter of aromatic-Cls formation under coexistence with a $CuCl_2$ catalyst upon heating at 400 °C. ∑CBzs and ∑PCBs in MFA-FePb at 400 °C also generated 1.6- and 1.7-times greater amounts of aromatic-Cls, respectively, than MFA-$FeCl_3$ (Table 2). Almost all congeners of CBzs and PCBs in MFA-FePb at 400 °C showed rate increases over 1.0, excluding the T3 congener of CBzs. Although a relatively high rate increase (FePb/Fe > 2.0) was detected only for the T4 congener of PCBs at 400 °C (Figure 3), rate increases of other congeners of CBzs and PCBs ranged from 1.4−1.9 without T3 congeners of CBzs (0.8), as shown in Table 2. The coexistence of $PbCl_2$ with $FeCl_3$ also promoted aromatic-Cls formation in the solid phase upon heating at 400 °C. In contrast, the gas phase did not indicate such promotion except for CBzs from MFA-CuPb (Table S2, Supporting Information). However, the total amounts of aromatic-Cls were influenced by the coexistence of $PbCl_2$.

In particular, the T4, P5, and H6 congeners of PCBs at 400 °C showed rate increases over 1.0 in MFA-CuPb and -FePb (Figure 3). The T4, P5, and H6 congeners of PCBs contained toxic isomers such as 3,3′,4,4′- (#77), 3,4,4′,5- (#81), 3,3′,4,4′,5- (#126), and 3,3′,4,4′,5,5′- (#169) chlorinated biphenyls, which were reported to have the relatively high toxicity equivalency factors (TEFs) of dioxins by the World Health Organization.[33] Table S5 (Supporting Information) lists that CuPb/Cu ratios of #77, #81, #126, and #169 PCBs resulted in values of 14, 3.2, 78, and 8.3, respectively, at 400 °C. Thus, the total equivalent quantity (TEQ) concentration derived from PCBs in MFA-CuPb (0.35 ng of TEQ/g) increased by 27 times compared to that in MFA-$CuCl_2$ (0.013 ng of TEQ/g). Toxic isomers #126 and #169 contributed 78.1% and 21.6% to the total TEQ concentration of MFA-CuPb at 400 °C. Compared with MFA-$FeCl_3$, MFA-FePb also exhibited increases of these toxic isomers, such as #77 (FePb/Fe = 1.4), #81 (1.1), #126 (1.2), and #169 (1.4) and the TEQ concentration from PCBs (1.3 ng of TEQ/g, FePb/Fe = 1.2) at 400 °C, as shown in Table S5 (Supporting Information). Toxic isomers #126 and #169 contributed 83.0% and 16.7% to the total TEQ concentration of MFA-FePb at 400 °C.

Coexistence of $PbCl_2$ Changes Dechlorination from Metal Catalysts. Quantitative GC/MS experiments revealed more effective promotion of aromatic-Cls formation by coexistence of $PbCl_2$ with other metal catalysts at 400 °C than at 300 °C. We performed Cl K-edge NEXAFS measurements to explore the thermochemical mechanism of $PbCl_2$ in the presence of other metal catalysts. Because we focused on chlorine bonded with heavy metals (lead, copper, and iron) and the carbon matrix, inorganic chlorine (KCl) was not added to the MFA for Cl K-edge NEXAFS analysis (Table S1, Supporting Information). According to a comparison of the measured spectrum with the theoretical spectrum, Cl K-edge NEXAFS analyses revealed an imbalance in the bonding state of chlorine caused by heating temperature.

For the MFA-[CuPb] series, the theoretical spectrum of (MFA-[Cu] + [Pb]) was calculated by linear combination of the spectra of MFA-[Cu] and -[Pb] at each temperature, as shown in panels a (300 °C) and b (400 °C) of Figure 4. In the theoretical calculations, the percentages of Cl derived from MFA-[Cu] and from MFA-[Pb] were 67% and 33%. At 300 °C, the measured spectrum of MFA-[CuPb] had a higher pre-edge at 2817 eV and a lower shoulder (2819−2820 eV) than the theoretical MFA-[Cu] + [Pb] spectrum (Figure 4a). The shape of the MFA-[CuPb] spectrum was closer to that of MFA-[Cu] at 300 °C. This suggests that the observed amount of chlorine bonded with copper was greater than the theoretical amount, which could decrease the dechlorination reaction from $CuCl_2$. As a result, the supply of chlorine from $CuCl_2$ for the generation of aromatic-Cls decreased. This might explain the lack of promotion of CBzs and the mild inhibition of PCBs by MFA-CuPb at 300 °C, as described above. The data in Figure 4b show that, at 400 °C, the spectrum of MFA-[CuPb] was more similar to that of MFA-[Pb] than to that of MFA-[Cu] + [Pb], based on the shoulder at 2819−2820 eV and the postedge structure (2822−2825 eV). The chlorine amounts bonded with Pb and Cu were higher and lower, respectively, than in the theoretical spectrum. Thus, the amount of dechlorination from $CuCl_2$ was higher at 400 °C, and the catalytic or direct chlorination[17,18] of carbon increased. At 400 °C, the promotion

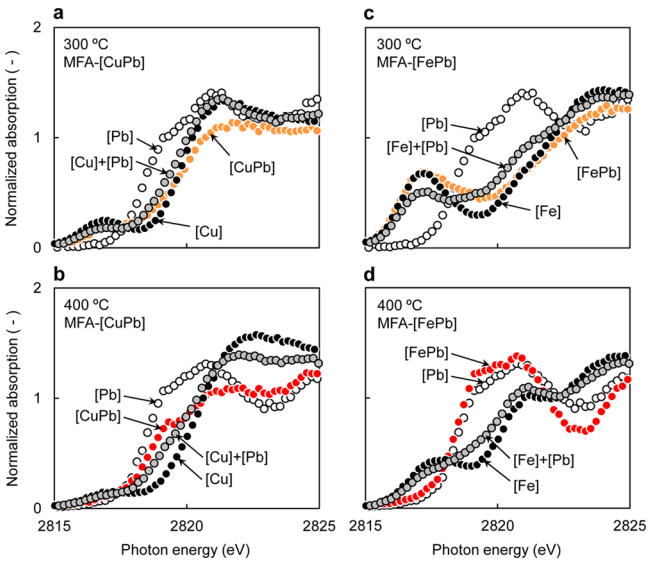

Figure 4. Cl K-edge NEXAFS spectra of various MFAs. MFA-[CuPb] after heating at (a) 300 and (b) 400 °C. MFA-[FePb] after heating at (c) 300 and (d) 400 °C. Reference spectra of MFA-[Cu], -[Fe], and -[Pb] after heating at each temperature are also shown. [Cu] + [Pb] and [Fe] + [Pb] indicate theoretical spectra generated by linear combinations of MFA-[Cu] and -[Fe], respectively, with MFA-[Pb].

of aromatic-Cls formation by coexistence of $PbCl_2$ with $CuCl_2$ (see Figure 3) was partly caused by the promotion of $CuCl_2$ dechlorination during the temperature increase from 300 to 400 °C.

Cl K-edge NEXAFS results for $PbCl_2$ coexisting with $FeCl_3$ (MFA-[FePb]) were also measured. The theoretical spectrum of MFA-[Fe] + [Pb] was calculated by a linear combination of the MFA-[Fe] and -[Pb] spectra at each temperature. In theoretical calculations, the percentages of Cl derived from MFA-[Fe] and from MFA-[Pb] were 72% and 28%, respectively. The thermochemical chlorine behavior in MFA-[FePb] showed tendencies similar to those of MFA-[CuPb]. MFA-[FePb] was closer to MFA-[Fe] at 300 °C (Figure 4c) and to MFA-[Pb] at 400 °C (Figure 4d) than MFA-[Fe] + [Pb]. Thus, the relatively mild inhibition of aromatic-Cls at 300 °C was caused in part by decreased $FeCl_3$ dechlorination. The promotion effect at 400 °C might be due to increased $FeCl_3$ dechlorination. The mechanism of thermochemical chlorination of carbon by $FeCl_3$ at 300−400 °C might be related to solid-phase oxychlorination.[21]

In the present study, we discussed the thermochemical role of Pb in aromatic-Cls formation in MSW fly ash in terms of both quantity and quality. When the only available chemical form of Pb in MSW fly ash is lead oxide, aromatic-Cls formation is suppressed by lead oxide. One possible mechanism of this suppression is partial chlorination of PbO from inorganic chlorine in the solid phase, based on the in situ Pb L_3-edge XANES data. In contrast, $PbCl_2$ promotes aromatic-Cls formation, to an extent that depends on the Pb concentration, heating temperature, and coexistence with other metal catalysts. We summarized two mechanisms of aromatic-Cls formation triggered by $PbCl_2$ in MSW fly ash. First, thermochemical partial oxidation of $PbCl_2$ within the temperature window (300−400 °C) is known to be important for the maximum formation of aromatic-Cls in MSW fly ash.[30] In particular, the real complex solid phase increased the thermochemical oxidation reactivity of $PbCl_2$, as determined using in situ Pb L_3-edge XANES spectroscopy. Second, GC/MS measurements and Cl K-edge NEAXFS analysis revealed the coexistence effect of $PbCl_2$ with other metal catalysts, such as $CuCl_2$ and $FeCl_3$. The relatively mild inhibition of aromatic-Cls at 300 °C is caused in part by decreased dechlorination by metal catalysts. Also, the promotion at 400 °C is caused by increased dechlorination by metal catalysts. Thus, the coexistence of $PbCl_2$ influences the imbalance of the bonding state of chlorine caused by heating temperature. In real MSW fly ash, Pb exists in both oxide and chloride forms. Therefore, aromatic-Cls formation depends on the balance between inhibition by lead oxide and promotion by lead chloride. Because Pb coexists with other metal catalysts in real MSW fly ash, the coexistence effect of $PbCl_2$ had to be considered. Overall, our mechanism-oriented study suggests that Pb in MSW fly ash functions as an "adjuster" in the generation of aromatic-Cls, depending on the lead oxide/chloride ratio and coexistence conditions with metal catalysts.

■ ASSOCIATED CONTENT

Ⓢ Supporting Information

Two descriptions and five tables, as mentioned in the text. This material is available free of charge via the Internet at http://pubs.acs.org.

■ AUTHOR INFORMATION

Corresponding Author

*E-mail: fujimori.takashi.3e@kyoto-u.ac.jp.

Notes

The authors declare no competing financial interest.

■ ACKNOWLEDGMENTS

We thank the staff and students of the Environmental Design Engineering Laboratory, Kyoto University, for help with in situ Pb L_3-edge XANES measurements; H. Tanida and T. Uruga (BL01B1) for support with Pb L_3-edge XANES measurements at SPring-8 (Proposals 2000B0309, 2001A0367, and 2004A0039); Y. Kitajima (BL-11B), Y. Inada (BL-9A), and K. Shiota for help with Cl K-edge NEXAFS measurements at the Photon Factory (Proposal 2007G069); Y. Nishimoto for additional GC/MS measurements under review. We acknowledge financial support from the Ministry of the Environment (K1632) and a Grant-in-Aid for Young Scientists (A) from JSPS (17681008).

■ REFERENCES

(1) Kawai, J.; Tohno, S.; Kitajima, Y.; Raola, O. E.; Takaoka, M. Depth selective chemical state analysis of Pb and S in fly ash in municipal solid waste incinerators using X-ray absorption spectroscopy. *Spectrochim. Acta B* **2003**, *58*, 635−639.

(2) Takaoka, M.; Yamamoto, T.; Tanaka, T.; Takeda, N.; Oshita, K.; Uruga, T. Direct speciation of lead, zinc and antimony in fly ash from waste treatment facilities by XAFS spectroscopy. *Phys. Scr.* **2005**, *T115*, 943−945.

(3) Yamamoto, H.; Nagoshi, M.; Yokoyama, T.; Takaoka, M.; Takeda, N. Investigation of chemical states for Pb of MSWI residues. *J. Jpn. Soc. Waste Manage. Experts* **2007**, *18*, 67−76 (in Japanese).

(4) Struis, R. P. W. J.; Nachtegaal, M.; Mattenberger, H.; Ludwig, C. The fate of lead in MSWI-fly ash during heat treatment: An X-ray absorption spectroscopy study. *Adv. Eng. Mater.* **2009**, *11*, 507−512.

(5) Nomura, Y.; Fujiwara, K.; Terada, A.; Nakai, S.; Hosomi, M. Prevention of lead leaching from fly ashes by mechanochemical treatment. *Waste Manage.* **2010**, *30*, 1290−1295.

(6) Funatsuki, A.; Takaoka, M.; Oshita, K.; Takeda, N. Methods of determining lead speciation in fly ash by X-ray absorption fine-structure spectroscopy and a sequential extraction procedure. *Anal. Sci.* **2012**, *28*, 481−490.
(7) Shah, P.; Strezov, V.; Nelson, P. F. X-ray absorption near edge structure spectrometry study of nickel and lead speciation in coals and coal combustion products. *Energy Fuels* **2009**, *23*, 1518−1525.
(8) Stieglitz, L.; Vogg, H. Carbonaceous particles in fly ash—A source for the formation of PCDD/PCDF in incineration process. *ISWA 88, Proc. Int. Solid Wastes Conf., 5th* **1988**, *1*, 331−335.
(9) Fujimori, T.; Takaoka, M.; Takeda, N. Influence of Cu, Fe, Pb and Zn chlorides and oxides on formation of chlorinated aromatic compounds in MSWI fly ash. *Environ. Sci. Technol.* **2009**, *43*, 8053−8059.
(10) Suzuki, K.; Kawamoto, K. Influence of chlorides and oxides on formation of chlorobenzenes by heating solid samples. *Proc. Annu. Conf. Jpn. Soc. Waste Manage. Experts, 14th* **2003**, 753−755 (in Japanese).
(11) Kokado, M.; Kamata, Y.; Kurata, M. Relationship between dioxins behavior and unburned carbon during exhaust gas treatment process − Catalytic effect of metals in fly ash by low-temperature oxidation of carbon. *Proc. Annu. Conf. Jpn. Soc. Waste Manage. Experts, 14th* **2003**, 747−749 (in Japanese).
(12) Qian, Y.; Zheng, M.; Liu, W.; Ma, X.; Zhang, B. Influence of metal oxides on PCDD/Fs formation from pentachlorophenol. *Chemosphere* **2005**, *60*, 951−958.
(13) Stach, J.; Pekaarek, V.; Endrst, R.; Hetflejs, J. Dechlorination of hexachlorobenzene on MWI fly ash. *Chemosphere* **1999**, *39*, 2391−2399.
(14) Yu, B.-W.; Jin, G.-Z.; Moon, Y.-H.; Kim, M.-K.; Kyoung, J.-D.; Chang, Y.-S. Emission of PCDD/Fs and dioxin-like PCBs from metallurgy industries in S. Korea. *Chemosphere* **2006**, *62*, 494−501.
(15) Ba, T.; Zheng, M.; Zhang, B.; Liu, W.; Su, G.; Xiao, K. Estimation and characterization of PCDD/Fs and dioxin-like PCB emission from secondary zinc and lead metallurgies in China. *J. Environ. Monit.* **2009**, *11*, 867−872.
(16) Farquar, G. R.; Alderman, S. L.; Poliakoff, E. D.; Dellinger, B. X-ray spectroscopic studies of the high temperature reduction of Cu(II) O by 2-chlorophenol on a simulated fly ash surface. *Environ. Sci. Technol.* **2003**, *37*, 931−935.
(17) Takaoka, M.; Shiono, A.; Nishimura, K.; Yamamoto, T.; Uruga, T.; Takeda, N.; Tanaka, T.; Oshita, K.; Matsumoto, T.; Harada, H. Dynamic change of copper in fly ash during de novo synthesis of dioxins. *Environ. Sci. Technol.* **2005**, *39*, 5878−5884.
(18) Fujimori, T.; Takaoka, M. Direct chlorination of carbon by copper chloride in a thermal process. *Environ. Sci. Technol.* **2009**, *43*, 2241−2246.
(19) Ryan, S. P.; Altwicker, E. R. Understanding the role of iron chlorides in the de novo synthesis of polychlorinated dibenzo-p-dioxins/dibenzofurans. *Environ. Sci. Technol.* **2004**, *38*, 1708−1717.
(20) Nganai, S.; Lomniski, S.; Dellinger, B. Ferric oxide formation of PCDD/Fs from 2-monochlorophenol. *Environ. Sci. Technol.* **2009**, *43*, 368−373.
(21) Fujimori, T.; Takaoka, M.; Morisawa, S. Chlorinated aromatic compounds in a thermal process promoted by oxychlorination of ferric chloride. *Environ. Sci. Technol.* **2010**, *44*, 1974−1979.
(22) Fujimori, T.; Tanino, Y.; Takaoka, M. Role of zinc in MSW fly ash during formation of chlorinated aromatics. *Environ. Sci. Technol.* **2011**, *45*, 7678−7684.
(23) Hinton, W. S.; Lane, A. M. Effect of zinc, copper, and sodium on formation of polychlorinated dioxins on MSW incinerator fly ash. *Chemosphere* **1992**, *25*, 811−819.
(24) Oberg, T.; Bergback, B.; Oberg, E. Different catalytic effects by copper and chromium on the formation and degradation of chlorinated aromatic compounds in fly ash. *Environ. Sci. Technol.* **2007**, *41*, 3741−3746.
(25) Oberg, T.; Bergback, B.; Filipsson, M. Catalytic effects by metal oxides on the formation and degradation of chlorinated aromatic compounds in fly ash. *Chemosphere* **2008**, *71*, 1135−1143.
(26) Kirby, C. S.; Rimstidt, J. D. Mineralogy and surface-properties of municipal solid waste ash. *Environ. Sci. Technol.* **1993**, *27*, 652−660.
(27) Eighmy, T. T.; Eusden, J. D., Jr.; Krzanowski, J. E.; Domingo, D. S.; Stampfli, D.; Martin, J. R.; Erickson, P. M. Comprehensive approach toward understanding element speciation and leaching behavior in municipal solid waste incineration electrostatic precipitator ash. *Environ. Sci. Technol.* **1995**, *29*, 629−646.
(28) Kida, A.; Noma, Y.; Imada, T. Chemical speciation and leaching properties of elements in municipal incinerator ashes. *Waste Manage.* **1996**, *16*, 527−536.
(29) Takaoka, M.; Yamamoto, T.; Shiono, A.; Takeda, N.; Oshita, K.; Matsumoto, T.; Tanaka, T. The effect of copper speciation on the formation of chlorinated aromatics on real municipal solid waste incinerator fly ash. *Chemosphere* **2005**, *59*, 1497−1505.
(30) Everaert, K.; Baeyens, J. The formation and emission of dioxins in large scale thermal processes. *Chemosphere* **2002**, *46*, 439−448.
(31) Fujimori, T.; Tanino, Y.; Takaoka, M.; Morisawa, S. Chlorination mechanism of carbon during dioxin formation using Cl-K near-edge X-ray-absorption fine structure. *Anal. Sci.* **2010**, *26*, 1119−1125.
(32) Addink, R.; Espourteille, F.; Altwicker, E. R. Role of inorganic chlorine in the formation of polychlorinated dibenzo-p-dioxins/dibenzofurans from residual carbon on incinerator fly ash. *Environ. Sci. Technol.* **1998**, *32*, 3356−3359.
(33) Van den Berg, M.; Birnbaum, L. S.; Denison, M.; De Vito, M.; Farland, W.; Feeley, M.; Fiedler, H.; Hakansson, H.; Hanberg, A.; Haws, L.; Rose, M.; Safe, S.; Schrenk, D.; Tohyama, C.; Tritscher, A.; Tuomisto, J.; Tysklind, M.; Walker, N.; Peterson, R. E. The 2005 World Health Organization reevaluation of human and mammalian toxic equivalency factors for dioxins and dioxin-like compounds. *Toxicol. Sci.* **2006**, *93*, 223−241.
(34) Takaoka, M.; Shiono, A.; Yamamoto, T.; Uruga, T.; Takeda, N.; Tanaka, T.; Oshita, K.; Matsumoto, T.; Harada, H. Relationship between dynamic change of copper and dioxin generation in various fly ash. *Chemosphere* **2008**, *73*, S78−S83.

NOTE ADDED AFTER ASAP PUBLICATION

Due to a production error, this paper published February 13, 2013 with an error in Table 2. The correct version published February 14, 2013.